Neurophotonics

Neurophotonics.SPIEDigitalLibrary.org

Short separation regression improves statistical significance and better localizes the hemodynamic response obtained by near-infrared spectroscopy for tasks with differing autonomic responses

Meryem A. Yücel
Juliette Selb
Christopher M. Aasted
Mike P. Petkov
Lino Becerra
David Borsook
David A. Boas

SPIE.

Short separation regression improves statistical significance and better localizes the hemodynamic response obtained by near-infrared spectroscopy for tasks with differing autonomic responses

Meryem A. Yücel,[a,*] Juliette Selb,[a] Christopher M. Aasted,[b] Mike P. Petkov,[b] Lino Becerra,[a,b,c] David Borsook,[a,b,c] and David A. Boas[a]
[a]Massachusetts General Hospital, Harvard Medical School, MGH/HST Athinoula A. Martinos Center for Biomedical Imaging, Department of Radiology, 149 13th Street, Charlestown, Massachusetts 02129, United States
[b]Boston Children's Hospital, Center for Pain and the Brain, Departments of Anaesthesia and Radiology, 300 Longwood Avenue, Boston, Massachusetts 02115, United States
[c]Harvard Medical School, Department of Anesthesiology, Perioperative, and Pain Medicine, 300 Longwood Avenue, Boston, Massachusetts 02115, United States

Abstract. Autonomic nervous system response is known to be highly task-dependent. The sensitivity of near-infrared spectroscopy (NIRS) measurements to superficial layers, particularly to the scalp, makes it highly susceptible to systemic physiological changes. Thus, one critical step in NIRS data processing is to remove the contribution of superficial layers to the NIRS signal and to obtain the actual brain response. This can be achieved using short separation channels that are sensitive only to the hemodynamics in the scalp. We investigated the contribution of hemodynamic fluctuations due to autonomous nervous system activation during various tasks. Our results provide clear demonstrations of the critical role of using short separation channels in NIRS measurements to disentangle differing autonomic responses from the brain activation signal of interest. [DOI: 10.1117/1.NPh.2.3.035005]

Keywords: functional near-infrared spectroscopy; autonomic nervous system; electrical stimulus; pain; finger tapping; systemic physiology.

Paper 15023RR received May 6, 2015; accepted for publication Aug. 10, 2015; published online Sep. 11, 2015.

1 Introduction

Near-infrared spectroscopy (NIRS) is a noninvasive imaging technique that is used to map the hemodynamic response associated with neuronal activity.[1,2] NIRS measures the changes in both oxygenated hemoglobin (HbO) and deoxygenated hemoglobin (HbR) using the intensity of near-infrared light measured between a source and a detector located on the skin.

The technique has found broad applications including studies of brain development,[3,4] functional connectivity,[5,6] cognitive science,[7,8] psychiatry and neurology,[9,10] aging,[11] and anesthesia.[12] The advantages of NIRS are the measurement of both HbO and HbR concentrations, its high-temporal resolution, low cost, and portability, while the disadvantages are low-spatial resolution and limited depth penetration.[13]

NIRS is a back-scattered measurement of the light that diffuses through the brain as well as the superficial layers: scalp and skull. The systemic physiological signals from superficial layers can have a larger magnitude than the brain signal itself.[13–15] Thus, the NIRS signal is mostly dominated by this systemic interference.[16] The major contributors of this interference are heartbeat, respiration, and low-frequency oscillations such as Mayer waves, as well as task-related changes in systemic physiology.[17] Thus, one critical step in NIRS data processing is to remove the contribution of superficial layers to the NIRS signal and to obtain the actual brain response.

Low-pass filtering is routinely used to remove cardiac oscillations;[18,19] however, it does not help with the lower frequency oscillations (0.2 Hz and slower). These lower frequency physiological fluctuations (including respiration, Mayer waves, and low and very low-frequency oscillations) significantly overlap with the hemodynamic response such that further filtering can remove the desired brain signal.[20] Various methods have been developed to overcome this issue. These methods include principal component analysis,[21] wavelet filtering,[22] adaptive average waveform subtraction,[23] subtraction of another NIRS source-detector channel performed over a nonactivated region of the brain,[18] multidistance NIRS measurements with layered models,[24] and using auxiliary recordings of global systemic physiology such as blood pressure.[25] A novel approach, developed relatively recently, is to use short separation detectors that are located in the activation area but have a shorter source-detector distance (less than one centimeter), and are thus more sensitive to superficial layers.[20,24,26–30] This approach assumes that the signal received at the short separation detector is mostly representative of the superficial layers, while the signal received at the long separation detector is sensitive to both the brain and the superficial layers. Thus, regressing out the short separation signal from the long separation signal effectively filters out the superficial component.

*Address all correspondence to: Meryem A. Yücel, E-mail: mayucel@nmr.mgh.harvard.edu

2329-423X/2015/$25.00 © 2015 SPIE

We have previously published the hemodynamic response to innocuous and noxious electrical pain and concluded that NIRS can be used as an objective measure of pain.[31] Here, we aimed to quantify the important contribution of using short separation regression in recovering the brain response and its localization. We demonstrate the impact that this superficial signal contamination can have on the interpretation of brain activation signals. We present measurements with three different stimuli: finger tapping and innocuous and noxious electrical stimulation. These stimuli produce different systemic physiological responses and demonstrate how regression using the short separation measurements can be critical for obtaining useful measurements of the brain activation signal.

2 Methods

The study was approved by the Institutional Review Board of the Massachusetts General Hospital and met the scientific and ethical guidelines of the Helsinki Accord and the International Association for the Study of Pain.[32]

2.1 *Probe and System*

Data were collected using a multichannel imager operating at 690 and 830 nm (TechEn Inc. Massachusetts, CW6 System). The probe contained 11 sources, 16 long separation detectors, and 11 short separation detectors. The source-detector distances used were approximately 3 cm for the long separation channels and 0.8 cm for the short separation channels. The probe covers portions of the somatosensory and motor areas on both hemispheres as well as the frontal cortex (Fig. 1). The results from the frontal region have been previously published.[31]

2.2 *Subjects and Experimental Design*

Eleven healthy subjects [right handed, male, 28 ± 5 (mean $\pm$ std) years old] were included in this study. A written consent was obtained from each subject prior to the experiments. Subjects with a history of neurological trauma or psychiatric disorders or who were unable to keep their head still throughout the experiment were excluded.

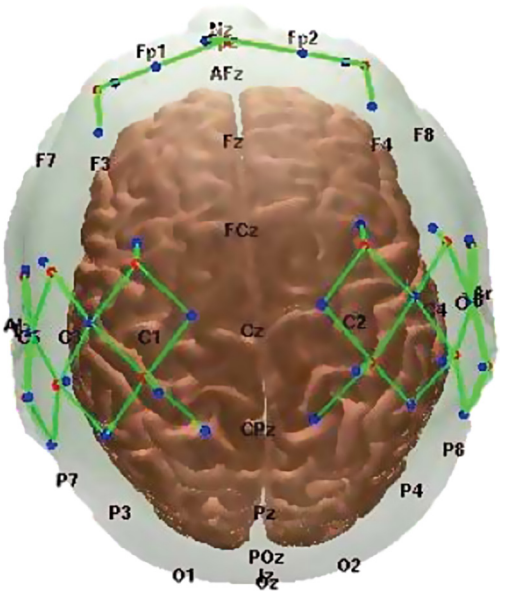

Fig. 1 Probe design. Sources (red circles), detectors (blue circles), channels (green lines) and EEG 10–20 reference points are shown. Figure made with AtlasViewer.[33]

Prior to the actual experiment, electrical stimulation was applied to each subject's left thumb through electrodes with a 5-Hz electrical stimulator (Neurometer CPT, Neurotron, Baltimore, Maryland) to determine current levels that elicited subjective pain ratings of 3/10 (innocuous) and 7/10 (noxious) from each subject. These personalized current values were used in the actual experiment.

Subjects first performed a left hand finger-tapping task (block design: 5 s on, 25 s off, repeated 12 times for a total of 6 min) during which NIRS measurements were recorded over the head. Following this, randomized innocuous and noxious electrical stimuli were applied. Each stimulus lasted 5 s, followed by a 25-s rest. Each run lasted 12.5 min and consisted of 12 innocuous and 12 noxious randomly ordered stimuli. The results shown in this paper are obtained from the first 3 min of the electrical run to avoid any habituation effect.[31]

2.3 *Analysis*

The NIRS channels with signals below a fixed noise level of 80 dB, or above a fixed saturation signal level of 140 dB on the TechEn CW6 were excluded from the analysis. The number of channels removed from the analysis varied between subjects, with between one and seven of the initial 51 channels being excluded. The signals were then converted into changes in optical density. The changes in HbO and HbR concentrations were then obtained using the modified Beer–Lambert law with a partial pathlength factor of six for both wavelengths.[13,34,35] Motion artifacts were detected using HOMER2[36] and the trials that contained motion artifacts within -2 to 15 s of the stimulus onset were excluded.

A general linear model, the details of which are explained below, was used for analysis with and without short separation regression. The signal at short separation channels are assumed to represent the superficial layers and the signal measured at the long separation channel is assumed to represent both brain tissue and the superficial layers. The systemic physiology extracted from short separation channels was used to regress out the systemic interference in the long separation channels.

The hemodynamic response function (HRF) [$h(t)$ in Eq. (1)] was modeled using a set of N_w consecutive Gaussian temporal basis functions [$b_i(t)$ with coefficients w_i in Eq. (1)] with a standard deviation of 0.5 s and their means separated by 0.5 s over the regression time range of -2 to 20 s, as we have previously used.[20] N_w stands for the number of basis functions used.

$$h(t) = \sum_{i=1}^{N_w} w_i b_i(t). \tag{1}$$

The HRF was then estimated by a general linear model approach that uses ordinary least squares. We used the standard block average estimator for the analysis without short separation [Eq. (2)] and the static simultaneous estimator for the analysis with short separation [Eqs. (2) and (3)]. y_{long} and y_{short} stand for the 3 and 0.8 cm separation channels, respectively. $u(t)$ is the stimulus onset vector with a value of one at the time of stimulus onset, and zero otherwise. N_a is the number of time points taken from the short separation channel in order to model the superficial signal in the long separation channel and a_i is the weight

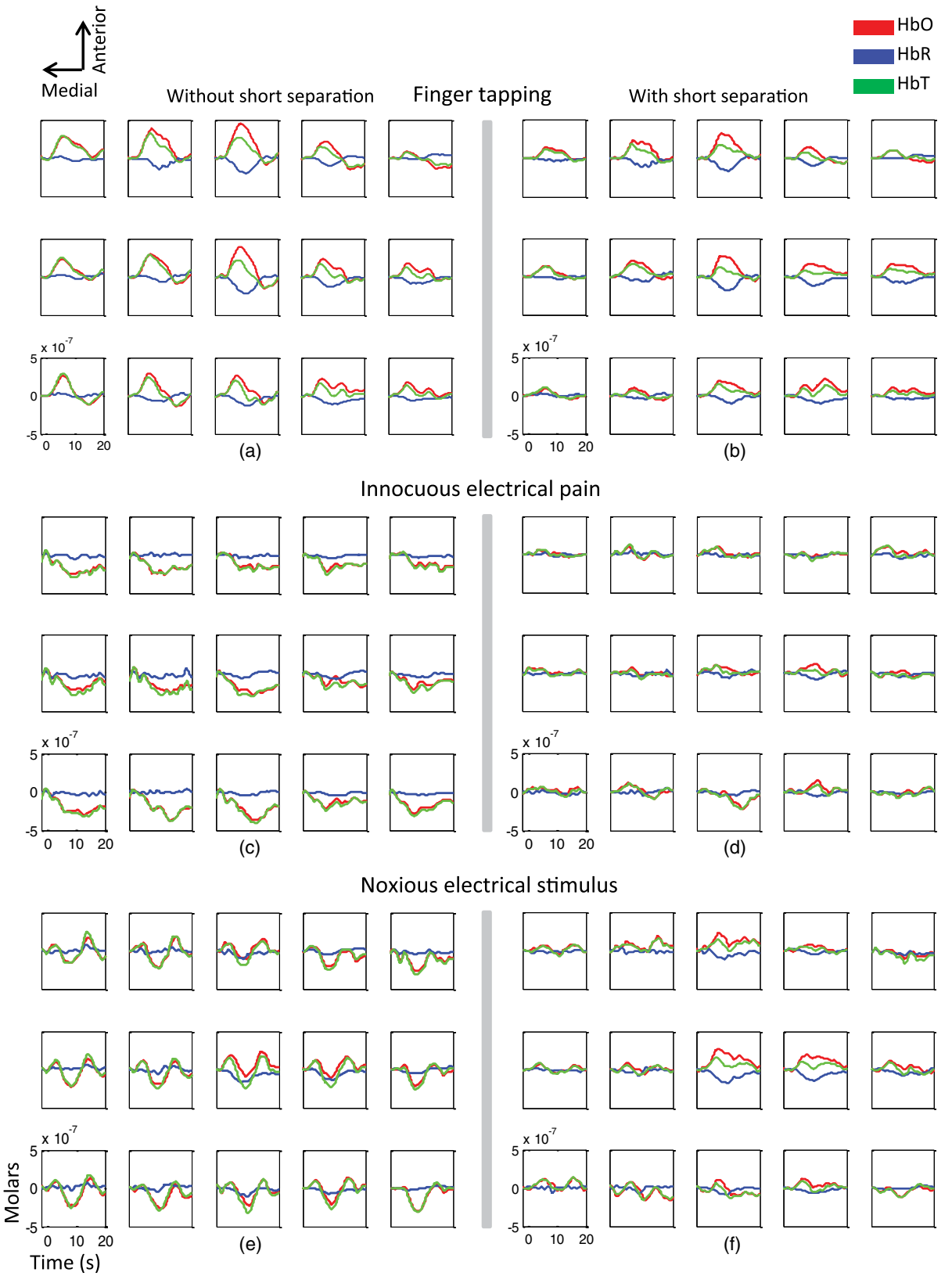

Fig. 2 Hemodynamic response to: (a) and (b) left hand finger tapping, (c) and (d) left thumb innocuous, (e) and (f) noxious electrical stimuli with and without short separation regression in right sensorimotor cortex. Group average results ($n = 11$) for the changes in HbO (red), HbR (blue), HbT (green). Note that figure panels (d), (e), and (f) are reproduced from our previous publication.[31]

used to model the superficial signal in the long separation channel.

$$y_{\text{long}}[t] = \sum_{k=-\infty}^{\infty} h(t)u(t-k), \tag{2}$$

$$y_{\text{long}}[t] = \sum_{k=-\infty}^{\infty} h(t)u(t-k) + \sum_{i=1}^{N_a} a_i y_{\text{short}}(t+1-i). \tag{3}$$

As for the short separation channel (y_{short}), the channel which had the highest correlation with a given long separation channel was used as a static estimator and regressed out from the long distance channel while simultaneously estimating the HRF as shown above (for further details, see Ref. 20). Analysis was carried out using the open source software HOMER2, which is implemented in MATLAB® (Mathworks, Natick, Massachusetts).

The heart rate was calculated for each subject from the 830-nm signal from a short separation channel by block averaging the heart rate during 0 to 10 s after stimulus for the task and 20 to 30 s after stimulus for the rest.

2.4 *Statistics and Spatial Dispersion*

A paired *t*-test was used to determine statistically significant differences in hemodynamic response (4 to 10 s after stimulus onset) from baseline (−2 to 0 s before stimulus) as well as differences in hemodynamic responses to innocuous and noxious stimuli. The significance level was chosen to be $p < 0.05$.

We have chosen a time range (4 to 10 s) that is representative of the hemodynamic response obtained (see Fig. 2) for *t*-maps and spatial-dispersion analysis.

Spatial dispersion was calculated as follows. The centroid coordinates (x_{centroid} and y_{centroid}) of the spatial region of the HRF in the contralateral hemisphere channels (a 3×5 matrix) were first calculated

$$x_{\text{centroid}} = \frac{\sum x_{\text{ch}} A_{\text{ch}}}{\sum A_{\text{ch}}} \qquad y_{\text{centroid}} = \frac{\sum y_{\text{ch}} A_{\text{ch}}}{\sum A_{\text{ch}}}, \tag{4}$$

where x_{ch} and y_{ch} are the coordinates of each channel (source-detector midpoint), and A_{ch} is the absolute value of the area under the curve of the HRF obtained for an individual channel within a specified time range (4 to 10 s after stimulus onset). That is, the location of the centroid was computed by weighting each channel location by the strength of the corresponding HRF.

The spatial dispersion was then calculated as

$$\sigma = \frac{\sum [(x_{\text{centroid}} - x_{\text{ch}})^2 + (y_{\text{centroid}} - y_{\text{ch}})^2]^{1/2} A_{\text{ch}}}{\sum A_{\text{ch}}}. \tag{5}$$

3 Results

Figure 2 depicts the group averaged HbO, HbR, and HbT (total hemoglobin) concentration changes in the contralateral sensorimotor cortex in response to finger tapping [panels (a) and (b)] and in response to innocuous [panels (c) and (d)] and noxious [panels (e) and (f)] electrical stimuli with and without short

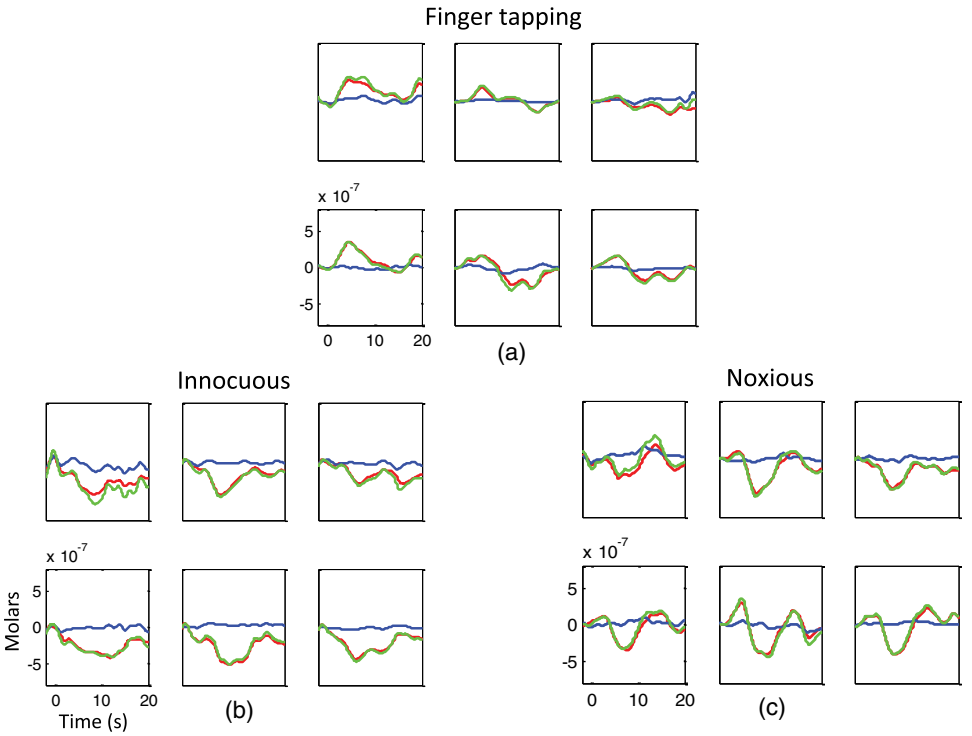

Fig. 3 Hemodynamic response in right sensorimotor cortex to: (a) left hand finger tapping, (b) left thumb innocuous, and (c) noxious electrical stimuli at short separation channels without short separation regression. Group average results ($n = 11$) for the changes in HbO (red), HbR (blue), HbT (green). Note that panel (c) is reproduced from our previous publication.[31]

separation regression. The hemodynamic responses for finger tapping obtained with and without using short separation regression look very similar [Figs. 2(a) and 2(b)], other than the spatial extent of the activation appears larger without the short separation regression. Further, the magnitude of the hemodynamic response is more localized by applying short separation regression. The short separation regression has a more dramatic effect on the hemodynamic response for innocuous and noxious electrical stimuli. Without using short separation regression, we observe a decrease in HbO or "deactivation" signal in all channels [Figs. 2(c) and 2(e)]. A well-localized, typical positive HRF, "activation" signal is only observed after the use of short separation regression [Fig. 2(d) and 2(f)]. These results imply that the global systemic response differs depending on the type of stimulus and indicate the dramatic impact that the systemic response can have on interpretation of the activation signal (i.e., positive versus negative signal changes) if not corrected.

Figure 3 shows the HbO, HbR, and HbT response in the right sensorimotor cortex to left hand finger tapping [Fig. 3(a)], innocuous and noxious electrical stimulus [Fig. 3(b)] at short separation channels. Finger tapping and noxious electrical stimuli result in hemodynamic responses in the scalp with different temporal characteristics. While the global systemic response for the finger tapping task is an increase in HbO and HbT [Fig. 3(a)], we observe a decrease for innocuous and noxious electrical stimuli [Figs. 3(b) and 3(c)]. There is an initial and a late positive peak surrounding the negative response for innocuous and noxious stimuli [Figs. 3(b) and 3(c)].

3.1 *Effect on Statistics: Short Separation Regression Increases Statistical Significance*

A paired t-test was performed to obtain the statistical significance of the difference between the changes in the HbO concentration averaged over the 4 to 10 s time interval after stimulus compared to the HbO concentration at baseline averaged from −2 to 0 s. The t-value statistical maps (t-maps) obtained are displayed in Fig. 4 [finger tapping without and with short separation regression [panels (a) and (b)], innocuous electrical stimulus without and with short separation regression [panels (c) and (d)] and noxious electrical stimulus without and with short separation regression [panels (e) and (f)]]. The statistical

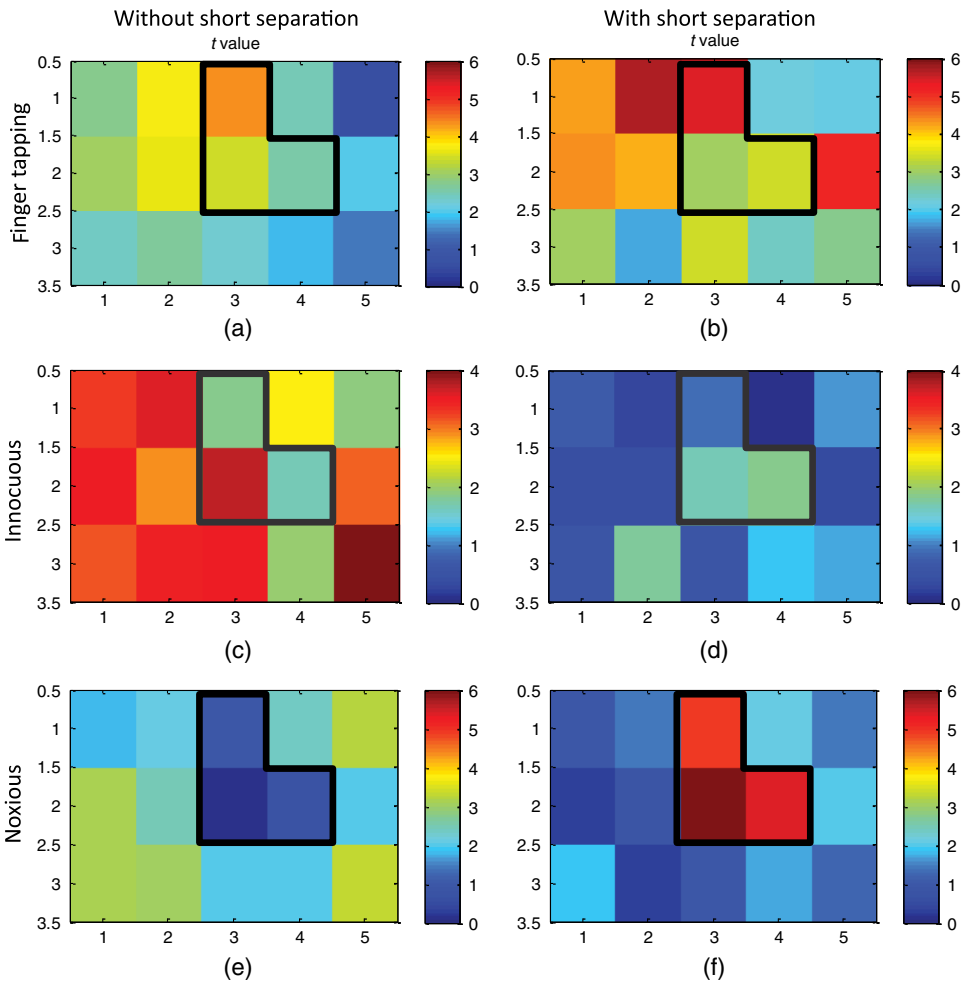

Fig. 4 The t-maps for the changes of HbO concentration from baseline [(a) and (b) finger tapping without and with short separation regression, (c) and (d) innocuous electrical, (e) and (f) noxious electrical]. The 3×5 grid corresponds to 3×5 channels in Fig. 2. The color bars show the t-value obtained by paired t-test. A t value of ~2 corresponds to $p = 0.05$. The squares surrounded by the black line covers the area of interest on the somatosensory and motor cortices where we expect to see a response.

significance obtained using short separation regression was higher for noxious electrical stimulus. The difference in statistical significance is relatively small for finger tapping. The significance of the innocuous response obtained without short separation was higher than with short separation [Figs. 4(c) and 4(d)], however, the response was distributed and is mostly not in the area of interest where a response is expected based on the underlying anatomy (area covered by the black line).

3.2 *Effect on Localization: Using Short Separation Regression Improves Localization and Decreases Spatial Dispersion*

A visual inspection of Figs. 4(c) and 4(d), which presents the statistical t-values for noxious electrical response without and with short separation regression, suggests that using short separation regression improves the localization of the hemodynamic response. A potential metric that can quantify the localization is the spatial dispersion of an image. Figure 5 presents the group average of spatial dispersion calculated for all 15 channels on the right hemisphere. There was a statistically significant decrease in the spatial dispersion of the hemodynamic response for the innocuous electrical stimulus after short separation regression. The decrease in spatial dispersion with regression for the noxious stimulus showed a trend toward significance.

3.3 *Effect on Statistics: Short Separation Regression is Necessary to Distinguish Noxious from Innocuous Electrical Stimulus*

Figure 6 compares the hemodynamic response to innocuous and noxious stimuli in the motor-sensory region without [panels (a) and (b)] and with [panels (c) and (d)] short separation regression. The HbO response to the noxious stimulus obtained using short separation regression was significantly higher than the response to the innocuous stimulus in the 4 to 6 s time range (paired t-test, $p = 0.008$). We used a short time range around the stimulus peak (5 s) for differentiating the two stimuli in order to perform our statistical analysis without any prior knowledge of the hemodynamic response. The statistical significance of the difference was reduced when no short separation regression was applied (paired t-test, $p = 0.02$).

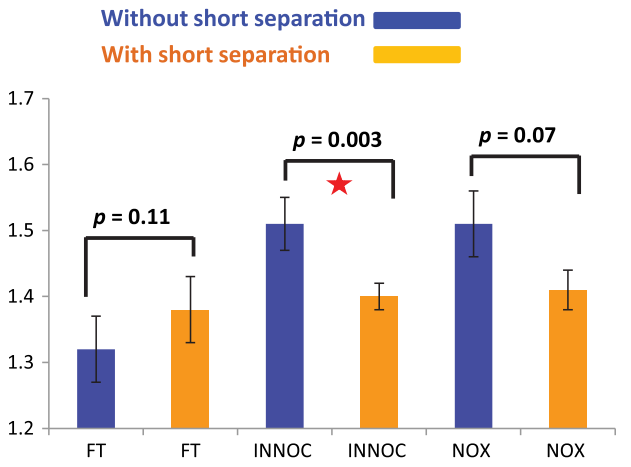

Fig. 5 Group average and standard error of the spatial dispersion on the contralateral hemisphere with (orange) and without (blue) short separation regression (FT: finger tapping; INNOC: innocuous; NOX: noxious). The p value lower than 0.05 (threshold for significance) is highlighted with a star.

The magnitude of the HbR response to noxious stimulus obtained using short separation regression was also significantly higher than the response to the innocuous stimulus [Fig. 7(c), paired t-test, $p = 0.002$]. The statistical significance was not affected by the regression of the systemic physiology [Fig. 7(a), paired t-test, $p = 0.003$]. Scatter plots show the difference in hemodynamic response between innocuous and noxious electrical stimuli for individual subjects [Figs. 6(b), 6(d), 7(b), and 7(d)].

4 Discussion

The autonomic nervous system is a control system that regulates many involuntary actions such as heart rate, respiration, and vasomotor activity. The system can be divided into sympathetic and parasympathetic nervous systems which are considered to be the "fight-or-flight" system and "rest and digest" system, respectively.[37] Both of these systems regulate blood vessels in different ways. Generally speaking, the sympathetic nervous system increases heart rate, respiration, blood pressure and results in peripheral vasoconstriction, while the parasympathetic nervous system works in the opposite direction.[38,39] The sympathetic and parasympathetic work synergistically and are both known to regulate the systemic response during a painful stimulus.[40]

The autonomic nervous system response is highly task-dependent (for the autonomic nervous system response during various tasks, see Refs. 17 and 41). While we observed a decrease in HbO levels for innocuous and noxious electrical stimulus when no short separation regression is applied, which is an indicator of a strong cephalic vasoconstriction [Figs. 3(b) and 3(c)], the finger-tapping task resulted in an increase in oxygenated hemoglobin in the scalp [Fig. 3(a)]. The changes observed due to innocuous and noxious electrical stimuli in short separation channels due to the systemic physiological response [Figs. 3(b) and 3(c)] were all statistically significant in their change from baseline (paired t-test, $p < 0.05$ for all short separation channels), while the changes were not found to be significant for finger tapping [Fig. 3(a)] (paired t-test, $p > 0.10$ for all short separation channels). These differences indicate that adding short separation channels to NIRS measurement is a critical step that allows distinguishing the scalp response from the brain response. While short separation channels capture the systemic response from the scalp, the long separation channels show a brain response integrated with a systemic response. Applying regression permits us to eliminate the responses observed at short separation channels, which are mainly due to activation of the autonomous system [Figs. 2(d) and 2(f)].

We have also obtained the heart rate both during rest and during the task periods for each type of stimulus. Our results show a statistically significant increase in heart rate during the finger tapping task as compared to rest [rest: 61.8 ± 2.2 BPM (beats per minute); finger tapping: 63.54 ± 2.05 BPM, $p = 0.009$ for paired t-test]. This result is consistent with previous literature.[18] While there was no significant change in heart rate due to either innocuous or noxious electrical stimuli, the tendency for noxious stimuli was toward a decline from baseline rather than an increase (rest: 61.7 ± 2.8 BPM; noxious: 60.7 ± 2.3 BPM, $p = 0.15$ for paired t-test; innocuous: 61.5 ± 2.7 BPM, $p = 0.85$ for paired t-test). Cardiac activity is under

the control of both sympathetic and parasympathetic branches of autonomous nervous system.[40,42] Thus, the difference between the global physiological responses during these two tasks may be attributed to the activation of a different autonomic system component that is driven by that specific task.

The combination of systemic vasoconstriction and deceleration of heart rate during a painful stimulus needs further discussion. While the autonomic response expected during a painful stimulus is a sympathetic response, hence an increase in heart rate and a cephalic vasoconstriction, the response is highly dependent on the stimulus intensity used in the experiment[43] which may result in two kinds of reflexes: orienting and defense. While the orienting reflex elicited by moderate intensity stimuli results in a deceleration of heart rate; the defensive reflex which is elicited by high-intensity stimuli accelerates it.[40] For example, Disbrow et al.[44] observed an increase in heart rate with electrical shock (6 beats per minute increase from baseline). However, the current level (20.8 mA) they used exceeded the current level we used for pain (maximum 5 mA). Our experimental pain stimulus seems to result in an orienting response, which is associated with a deceleration of heart rate and cephalic vasoconstriction.[45,46]

One interesting observation was that the statistical *t*-maps for the finger tapping task obtained by averaging the time window of 4 to 6 s after stimulus presentation have the highest *t*-value located in the channels more medial compared to the channels with the most significant activation obtained from the *t*-maps by averaging the time window of 5 to 12 s of the hemodynamic response profile (figure not shown). This implies that the location of the most statistically significant response changes in time throughout the hemodynamic response, an observation that is difficult to see if no regression is applied. This could either be showing the flow of blood to the area where neuronal activation takes place, or it could be due to the interplay between the brain response and sympathetic nervous system response.

Another interesting point is the effect of short separation regression on oxyhemoglobin in comparison to that on deoxyhemoglobin. Unlike the dramatic change observed in the HbO response by applying short separation regression, the HbR response was relatively unaltered (Figs. 6 and 7). The HbR change on short separation channels were also much smaller compared to the HbO change (Fig. 3). A similar observation was also made by Kirilina et al.[17] One possible explanation is that while arteries, arterioles, and veins are innervated by the autonomic nervous system, the venules and capillaries, where most of the HbR concentration change is happening, are not.[43] Thus, the effect of the activation of the sympathetic nervous system is mostly observed on the HbO response.

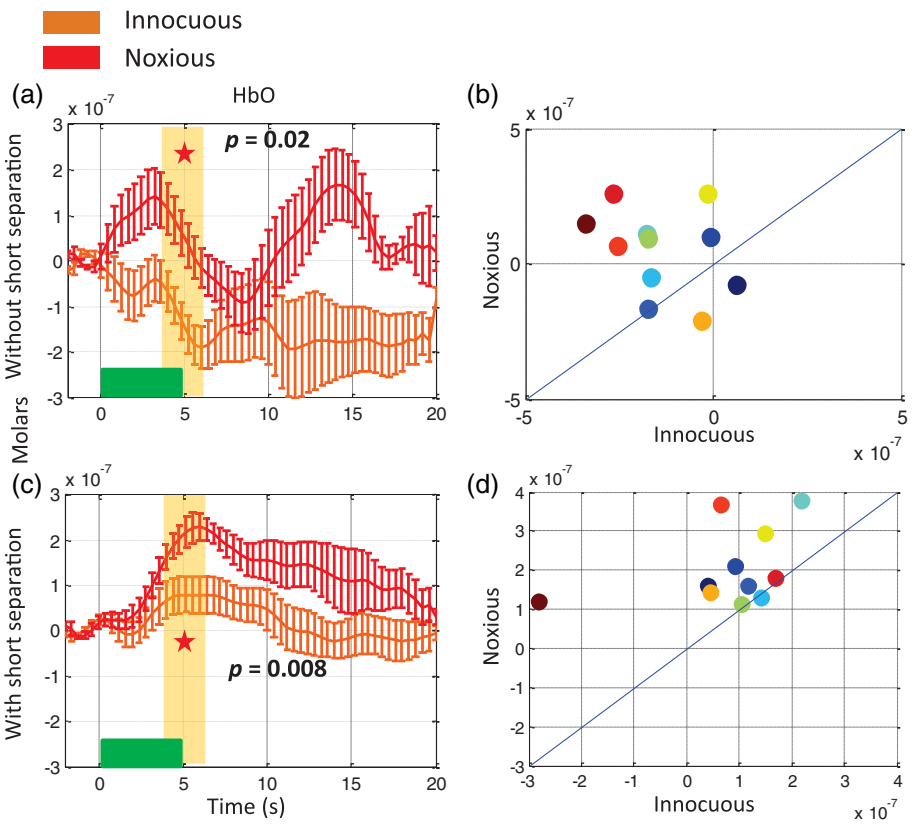

Fig. 6 Comparison of the hemodynamic response in the right sensorimotor cortex to left-thumb innocuous and noxious stimuli. Changes in HbO as a response to innocuous stimuli (orange) and noxious stimuli (red) obtained (a) without and (c) with short separation regression. The horizontal green bar shows the stimulus duration. Yellow bars show the interval chosen to obtain the mean responses depicted in the scatter plots and stars indicate a statistically significant difference ($p < 0.05$). *P*-value is obtained using a paired *t*-test that compares the yellow highlighted time interval and baseline. The panels (b) and (d) show a scatter plot comparing the hemodynamic response amplitude for each subject averaged over the yellow bar. Note that panels (c) and (d) are reproduced from our previous publication.[31]

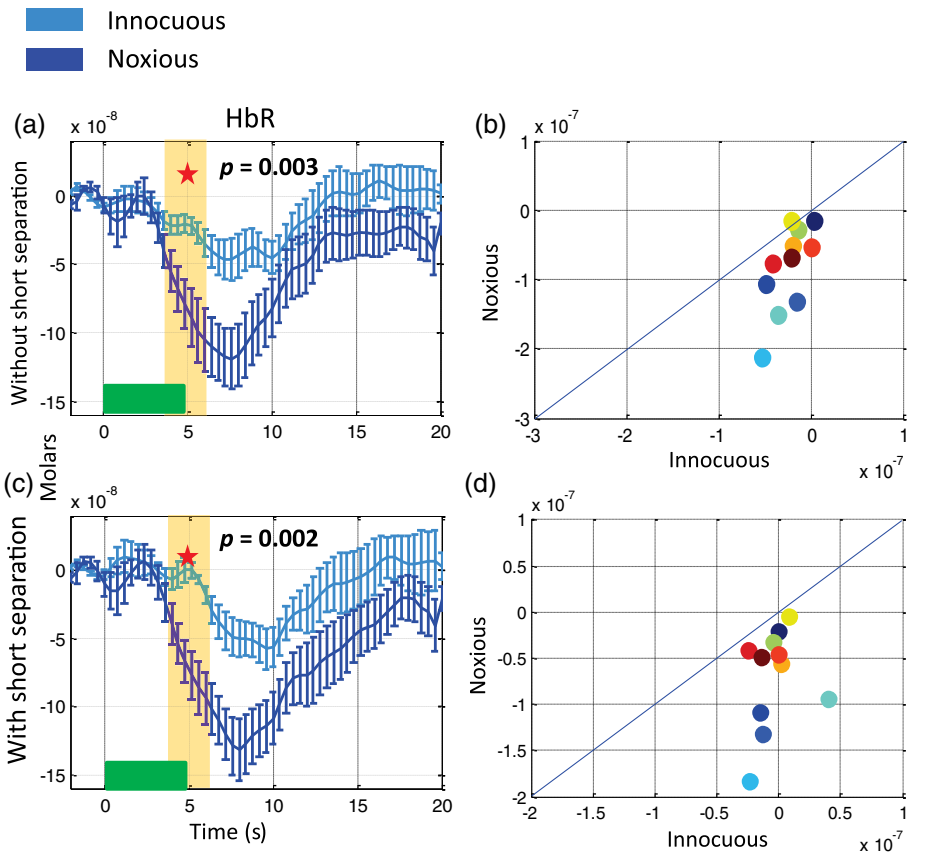

Fig. 7 Comparison of the hemodynamic response in the right sensorimotor cortex to innocuous and noxious stimuli. Changes in HbO as a response to innocuous stimuli (light blue) and noxious stimuli (dark blue) obtained (a) without and (c) with short separation regression. The horizontal green bar shows the stimulus duration. Yellow bars show the interval chosen to obtain the mean response amplitudes depicted in the scatter plots and stars indicate a statistically significant difference ($p < 0.05$). *P*-value is obtained using a paired *t*-test that compares the yellow highlighted time interval and baseline. The panels (b) and (d) show a scatter plot comparing the hemodynamic response amplitude for each subject averaged over the yellow bar. Note that panels (c) and (d) are reproduced from our previous publication.[31]

5 Conclusion

NIRS is a back-scattering measurement of the light that diffuses through the brain as well as the scalp and the skull. Thus, the NIRS signal obtained is an integration of the brain signals from cortex as well as the systemic physiological signals from superficial layers. Therefore, one important step in NIRS data processing is to remove the contribution of superficial layers to the NIRS signal and to extract the actual brain response. Especially with experimental tasks that trigger the autonomic nervous system such as pain, it becomes more critical to distinguish the brain response from the scalp. This work shows that different stimuli elicit different systemic effects. Importantly, we also demonstrated that using short separation channels makes it possible to extract the underlying brain response that is otherwise hidden by the sympathetic response.

Acknowledgments

This work was supported by the National Institutes of Health through Grants P41-EB015896, R01-EB006385, and R01-GM104986. The content is solely the responsibility of the authors and does not necessarily represent the official views of the National Institutes of Health. Competing financial interests: D.A.B. is an inventor on a technology licensed to TechEn, a company whose medical pursuits focus on noninvasive optical brain monitoring. D.A.B.'s interests were reviewed and are managed by Massachusetts General Hospital and Partners HealthCare in accordance with their conflict of interest policies.

References

1. F. F. Jobsis, "Noninvasive infrared monitoring of cerebral and myocardial sufficiency and circulatory parameters," *Science* **198**(4323), 1264–1267 (1997).
2. A. Villringer et al., "Near infrared spectroscopy (NIRS): a new tool to study hemodynamic changes during activation of brain function in human adults," *Neurosci. Lett.* **154**(1–2), 101–104 (1993).
3. R. E. Vanderwert and C. A. Nelson, "The use of near-infrared spectroscopy in the study of typical and atypical development," *NeuroImage* **85**(1), 264–271 (2014).
4. N. Roche-Labarbe et al., "Somatosensory evoked changes in cerebral oxygen consumption measured non-invasively in premature neonates," *NeuroImage* **85**(1), 279–286 (2014).
5. M. Imai et al., "Functional connectivity of the cortex of term and preterm infants and infants with Down's syndrome," *NeuroImage* **85**(1), 272–278 (2014).
6. A. V. Medvedev, "Does the resting state connectivity have hemispheric asymmetry? A near-infrared spectroscopy study," *NeuroImage* **85**(1), 400–407 (2014).
7. G. Fu et al., "The neural correlates of the face attractiveness aftereffect: a functional near-infrared spectroscopy (fNIRS) study," *NeuroImage* **85**(1), 363–371 (2014).

8. S. B. Perlman et al., "fNIRS evidence of prefrontal regulation of frustration in early childhood," *NeuroImage* **85**(1), 326–334 (2014).
9. R. Takizawa et al., "Neuroimaging-aided differential diagnosis of the depressive state," *NeuroImage* **85**(1), 498–507 (2014).
10. H. Fujimoto et al., "Cortical changes underlying balance recovery in patients with hemiplegic stroke," *NeuroImage* **85**(1), 547–554 (2014).
11. M. Fabiani et al., "Neurovascular coupling in normal aging: a combined optical, ERP and fMRI study," *NeuroImage* **85**(1), 592–607 (2014).
12. A. Curtin et al., "Functional near-infrared spectroscopy for the measurement of propofol effects in conscious sedation during outpatient elective colonoscopy," *NeuroImage* **85**(1), 626–636 (2014).
13. D. A. Boas, A. M. Dale, and M. A. Franceschini, "Diffuse optical imaging of brain activation: approaches to optimizing image sensitivity, resolution, and accuracy," *NeuroImage* **23**(Suppl. 1), S275–S288 (2004).
14. H. Obrig et al., "Spontaneous low frequency oscillations of cerebral hemodynamics and metabolism in human adults," *NeuroImage* **12**, 623–639 (2000).
15. V. Toronov et al., "Near-infrared study of fluctuations in cerebral hemodynamics during rest and motor stimulation: temporal analysis and spatial mapping," *Med. Phys.* **27**, 801–815 (2000).
16. C. Mansouri et al., "Depth sensitivity analysis of functional near-infrared spectroscopy measurement using three-dimensional Monte Carlo modelling-based magnetic resonance imaging," *Lasers Med. Sci.* **25**(3), 431–438 (2010).
17. E. Kirilina et al., "The physiological origin of task-evoked systemic artefacts in functional near infrared spectroscopy," *NeuroImage* **61**(1), 70–81 (2012).
18. M. A. Franceschini et al., "Hemodynamic evoked response of the sensorimotor cortex measured noninvasively with near-infrared optical imaging," *Psychophysiology* **40**(4), 548–560 (2003).
19. G. Jasdzewski et al., "Differences in the hemodynamic response to event-related motor and visual paradigms as measured by near-infrared spectroscopy," *NeuroImage* **20**(1), 479–488 (2003).
20. L. Gagnon et al., "Improved recovery of the hemodynamic response in diffuse optical imaging using short optode separations and state-space modeling," *NeuroImage* **56**(3), 1362–1371 (2011).
21. Q. Zhang et al., "Eigenvector-based spatial filtering for reduction of physiological interference in diffuse optical imaging," *J. Biomed. Opt.* **10**(1), 011014 (2005).
22. J. M. Lina et al., "Complex wavelets applied to diffuse optical spectroscopy for brain activity detection," *Opt. Express* **16**(2), 1029–1050 (2008).
23. G. Gratton and P. M. Corballis, "Removing the heart from the brain: compensation for the pulse artifact in the photon migration signal," *Psychophysiology* **32**(3), 292–299 (1995).
24. S. Umeyama and T. Yamada, "Monte carlo study of global interference cancellation by multidistance measurement of near-infrared spectroscopy," *J. Biomed. Opt.* **14**(6), 064025 (2009).
25. I. Tachtsidis et al., "Functional optical topography analysis using statistical parametric mapping (SPM) methodology with and without physiological confounds," *Adv. Exp. Med. Biol.* **662**, 237–243 (2010).
26. R. B. Saager and A. J. Berger, "Measurement of layer-like hemodynamic trends in scalp and cortex: implications for physiological baseline suppression in functional near infrared spectroscopy," *J. Biomed. Opt.* **13**(3), 034017 (2008).
27. Q. Zhang, E. N. Brown, and G. E. Strangman, "Adaptative filltering for global interference cancellation and real-time recovery of evoked brain activity: a Monte Carlo simulation study," *J. Biomed. Opt.* **12**(4), 044014 (2007).
28. Q. Zhang, E. N. Brown, and G. E. Strangman, "Adaptative filtering to reduce global interference in evoked brain activity detection: a human subject case study," *J. Biomed. Opt.* **12**(6), 064009 (2007).
29. T. Yamada, S. Umeyama, and K. Matsuda, "Multidistance probe arrangement to eliminate artifacts in functional near-infrared spectroscopy," *J. Biomed. Opt.* **14**(6), 064034 (2009).
30. N. M. Gregg et al., "Brain specificity of diffuse optical imaging: improvements from superficial signal regression and tomography," *Front. Neuroenerg.* **2**(14), 1–8 (2010).
31. M. A. Yücel et al., "Specificity of hemodynamic brain responses to painful stimuli: a functional near-infrared spectroscopy study," *Sci. Rep.* **5**, 9469 (2015).
32. "WMA declaration of Helsinki - Ethical principles for medical research involving human subjects," *64th WMA General Assembly*, Fortaleza, Brazil, October 2013 http://www.wma.net/en/30publications/10policies/b3/.
33. C. M. Aasted et al., "Anatomical guidance for functional near-infrared spectroscopy: AtlasViewer tutorial," *Neurophotonics* **2**(2), 020801 (2015).
34. M. Cope and D. T. Delpy, "System for long-term measurement of cerebral blood and tissue oxygenation on newborn infants by near infra-red transillumination," *Med. Biol. Eng. Comput.* **26**, 289–294 (1988).
35. D. T. Delpy et al., "Estimation of optical pathlength through tissue from direct time of flight measurement," *Phys. Med. Biol.* **33**, 1433–1442 (1988).
36. T. J. Huppert et al., "HomER: a review of time-series analysis methods for near-infrared spectroscopy of the brain," *Appl. Opt.* **48**, D280–D298 (2009).
37. L. K. McCorry, "Physiology of the autonomic nervous system," *Am. J. Pharm. Educ.* **71**(4), 78 (2007)
38. J. A. Bevan and J. E. Brayden, "Nonadrenergic neural vasodilator mechanisms," *Circ. Res.* **60**, 309–326 (1987).
39. B. N. Kyle and D. W. McNeil, "Autonomic arousal and experimentally induced pain: a critical review of the literature," *Pain Res. Manage.* **19**(3), 159–167 (2014).
40. W. Janig and H. J. Habler, "Organization of the autonomic nervous system: structure and function," in O. Appenzeller, Ed., *Handbook of Clinical Neurology*, Vol. 74 (30), The Autonomic Nervous System. Part 1. Normal Functions, pp. 1–52, Elsevier, Amsterdam (1999).
41. T. Takahashi et al., "Influence of skin blood flow on near-infrared spectroscopy signals measured on the forehead during a verbal fluency task," *NeuroImage* **57**(3), 991–1002 (2011).
42. G. D. Thomas, "Neural control of the circulation," *AJP Adv. Physiol. Educ.* **35**(1), 28–32 (2011).
43. G. Turpin, "Effects of stimulus intensity on autonomic responding: the problem of differentiating orienting and defense reflexes," *Psychophysiology* **23**(1), 1–14 (1986).
44. E. Disbrow et al., "Somatosensory cortex: a comparison of the response to noxious thermal, mechanical, and electrical stimuli using functional magnetic resonance imaging," *Hum. Brain Mapp.* **6**(3), 150–159 (1998).
45. G. Turpin and D. A. Siddle, "Effects of stimulus intensity on cardiovascular activity," *Psychophysiology* **20**(6), 611–624 (1983).
46. G. Turpin, F. Schaefer, and W. Boucsein, "Effects of stimulus intensity, risetime, and duration on autonomic and behavioral responding: implications for the differentiation of orienting, startle, and defense responses," *Psychophysiology* **36**(4), 453–463 (1999).

Meryem A. Yücel majored in chemical engineering at Boğaziçi University, İstanbul. She received her PhD in biomedical engineering from the Biomedical Engineering Institute, Boğaziçi University, İstanbul. She is currently an instructor at Harvard Medical School at the Athinoula A. Martinos Center for Biomedical Imaging and assistant in biomedical engineering at Massachusetts General Hospital. Her research interests include neurovascular coupling and brain imaging using various modalities.

Juliette Selb received her PhD from the Université Paris Sud in France for her work on acousto-optic imaging. She is an instructor in the Optics Division of the Athinoula A. Martinos Center for Biomedical Imaging at Massachusetts General Hospital, Harvard Medical School. Her current research focuses on diffuse optical modalities for brain imaging in humans.

Christopher M. Aasted studied engineering at the Colorado School of Mines before receiving his MS degree in mechatronic systems engineering and his PhD in engineering from the University of Denver. His research has focused on intelligent control systems and other machine learning applications in both biomedical signal processing and unmanned aerial systems. He is currently an instructor at Harvard Medical School and a staff scientist at Boston Children's Hospital.

Mike P. Petkov is a clinical research assistant at Boston Children's Hospital and Massachusetts General Hospital. He graduated from Boston University in 2012 with a Bachelor of Arts in chemistry and a minor in mathematics. He is involved in NIRS studies involving healthy controls and patients under anesthesia. He is also involved

in PET-fMRI studies involving the placebo effect of migraine subjects and neuroinflammation of spinal cord injury subjects.

Lino Becerra studied physics at Universidad Nacional de Ingenieria in Peru. He obtained his PhD in physics from the University of Illinois Urbana-Champaign. His research has focused in the understanding of pain processing in the brain through neuroimaging techniques, including diffuse optical imaging and magnetic resonance. He is an associate professor at the Harvard Medical School and codirector of the Center for Pain and the Brain.

David Borsook is a neurologist and neurobiologist by training. He received his MD and PhD degrees from the University of Witwatersrand, South Africa. Currently, he directs the Center for Pain and the Brain and consults for a number of pharmaceutical and biotechnology companies in the fields of pain, analgesics, and imaging. He is a professor at Harvard Medical School and has appointments at McLean Hospital (psychiatry), Massachusetts General Hospital (radiology/psychiatry), and Boston Children's Hospital (anesthesiology/radiology).

David A. Boas is the director of the Martinos Optics Division in the Department of Radiology at the Massachusetts General Hospital and a professor at the Harvard Medical School. He received his PhD in physics from the University of Pennsylvania. His research focuses on developing novel optical methods to study cerebral physiology and pathophysiology focusing on studying brain function, oxygen delivery, and consumption. He is the founding president of the Society for Functional Near-Infrared Spectroscopy.